Cell Biol Toxicol (2012) 28:47–56
DOI 10.1007/s10565-011-9204-8

Andrographolide induces cell cycle arrest and apoptosis in human rheumatoid arthritis fibroblast-like synoviocytes

Jie Yan · Yang Chen · Chao He · Zhen-zhen Yang · Cheng Lü · Xin-shan Chen

Received: 31 May 2011 / Accepted: 27 September 2011 / Published online: 20 October 2011

Abstract The pseudo-tumoral expansion of fibroblast-like synoviocytes is a hallmark of rheumatoid arthritis (RA), and targeting rheumatoid arthritis fibroblast-like synoviocytes (RAFLSs) may have therapeutic potentials in this disease. Andrographolide, a diterpenoid compound isolated from the herb *Andrographis paniculata*, has been reported to have potent anti-inflammatory activity. In the present study, we aimed to investigate the effects of andrographolide on human RAFLSs and the underlying molecular mechanism(s). RAFLSs were isolated from patients with RA and treated with or without various concentrations (i.e., 10, 20, and 30 μM) of andrographolide for 48 h. 3-[4,5-Dimethyl-2-yl]-2,5-diphenyl tetrazolium bromide assay revealed that andrographolide treatment decreased the proliferation of RAFLSs in a dose-dependent manner. Cell cycle analysis using propidium iodide (PI) staining showed a G0/G1 cell cycle arrest in andrographolide-treated RAFLSs. Immunoblotting analysis of key cell cycle regulators demonstrated that andrographolide treatment caused a dose-dependent increase in the expression of cell-cycle inhibitors p21 and p27 and a concomitant reduction of cyclin-dependent kinase 4. Exposure to andrographolide-induced apoptosis of RAFLSs measured by annexin V/PI double staining, which was coupled with promotion of cytochrome C release from mitochondria and activation of caspase-3. Moreover, andrographolide-treated RAFLSs displayed a significant decrease in the Bcl-2/Bax ratio compared to untreated cells. In conclusion, our data demonstrate that andrographolide exerts anti-growth and pro-apoptotic effects on RAFLSs, thus may have therapeutic potential for the treatment of RA.

Keywords Rheumatoid arthritis fibroblast-like synoviocytes (RAFLSs) · Andrographolide · Cell viability · Cell cycle · Apoptosis

J. Yan · Y. Chen · C. He · Z.-z. Yang · C. Lü · X.-s. Chen (✉)
Faculty of Forensic Medicine, Tongji Medical College, Huazhong University of Science and Technology, Wuhan 430030, China
e-mail: chenxlsci@yahoo.cn

Introduction

Rheumatoid arthritis (RA) is an autoimmune disease characterized by synovial hyperplasia and cartilage degradation (Firestein 2003). The aggressive front of synovial tissue, termed pannus, invades and destroys the local articular structure (Firestein 2003; Pope 2002). The pannus is mainly composed of fibroblast-like synoviocytes (FLSs) combined with a massive infiltration of lymphocytes and macrophages. FLSs in patients with RA (RAFLSs) differ substantially from normal FLSs; the former undergo a distinct set of morphological and biological changes to acquire an aggressive, invasive phenotype commonly associated with transformed cells (Firestein 1996). RAFLSs can grow in an anchorage-independent manner in soft

agarose (Lafyatis et al. 1989) and have the capacity to attach to and deeply invade the articular cartilage in a mouse model of RA (Müller-Ladner et al. 1996). It is well established that activated FLSs play an important role in the pathogenesis of RA through release of proinflammatory cytokines and matrix-degrading enzymes (Pap et al. 2000). Targeting RAFLSs is thus believed to exert therapeutic effects on RA.

Andrographolide is a diterpenoid lactone isolated from an herbaceous plant *Andrographis paniculata*. This compound is known to possess strong anti-inflammatory and antiviral properties (Bao et al. 2009; Chen et al. 2009; Li et al. 2009). Andrographolide attenuates allergic asthma via inhibition of the nuclear factor-kappaB (NF-κB) signaling pathway (Bao et al. 2009). Andrographolide also has anti-cancer activity. It has been reported that andrographolide inhibits cell viability and induces apoptotic cell death in both androgen-stimulated and castration-resistant human prostate cancer cells through interfering with the interleukin-6-mediated signaling (Chun et al. 2010). Manikam and Stanslas (2009) found that andrographolide exhibits strong growth inhibitory activity in acute promyelocytic leukemia NB4 cells. Recently, a prospective randomized placebo-controlled trial has suggested that *A. paniculata* is effective for symptom relief in patients with RA (Burgos et al. 2009). In view of these findings, here we investigated the effects of andrographolide on RAFLSs and the potential molecular mechanism(s) involved.

Materials and methods

Antibodies and reagents

Primary antibodies used for immunoblotting analysis were as follows: antibodies against Bax (1:1,000, #5023), Bcl-2 (1:1,000, #2872), and cleaved caspase 3 (1:1,000, #9661) were purchased from Cell Signaling Technology (Beverly, MA, USA); anti-cyclin-dependent kinase (Cdk)4 (1:500, sc-56277), anti-p27 (1:500, sc-53906), anti-p21 (1:500, sc-469), anti-cytochrome C (1:500, sc-65396), and β-actin (1:2000, sc-130301) were purchased from Santa Cruz Biotechnology (Santa Cruz, CA, USA); anti-pro-caspase-3 (1:100, ab13586) was obtained from Abcam (Cambridge, MA, USA). Horseradish peroxidase-linked secondary antibodies were obtained from Santa Cruz Biotechnology. Anti-CD3-PE (#555340), anti-CD14-FITC (#555397), anti-CD19-APC (#555415), and anti-CD90-FITC (#555595) were purchased from BD Biosciences (San Diego, CA, USA). Andrographolide and 3-[4,5-dimethyl-2-yl]-2,5-diphenyl tetrazolium bromide (MTT)@ were purchased from Sigma (St. Louis, MO, USA).

Isolation and culture of RAFLSs

The study protocol was approved by the Ethics Committee of Huazhong University of Science and Technology (Wuhan, China). Fibroblasts were isolated from synovium obtained from 15 patients with RA (Arnett et al. 1988) who had undergone total joint replacement surgery. The main clinical characteristics of the RA patients are indicated in Table 1. The 15 patients were randomly divided into 3 subsets (n=5 for each subset), and synovial tissues collected from each subset were pooled together prior to the isolation of FLSs. Fresh synovial tissues were chopped into fragments of less than 1 mm, washed extensively in sterile phosphate-buffered saline (PBS), and digested with 1 mg/mL collagenase 1 (Sigma) in PBS for 2 h at 37°C under continuous agitation. The resulting cell suspension was filtered through a 70 μm cell strainer, and cultured in 75 cm^2 culture flasks with Dulbecco's modified Eagle's medium (DMEM; Invitrogen, Carlsbad, CA, USA) containing 10% fetal calf serum (FCS; Invitrogen) and antibiotics (100 U/mL penicillin, 100 μg/mL streptomycin) at 37°C in an atmosphere of 5% CO_2. The culture medium was replaced every 3 days. When confluent, cells were passaged at 1:3 dilutions. The cells were morphologically homogeneous and exhibited the appearance of synovial fibroblasts, with typical bipolar configuration

Table 1 Clinical characteristics of the RA patients (n=15)

Clinical variables	
Male/female (n)	3/12
Mean age (years), mean (±SD)	60 (±9)
Body mass index (kg/m^2), mean (±SD)	21.5 (±2.8)
CRP (mg/dl), median (range)	2.0 (0.4–9.0)
RF positivity, %	73
RF (IU/ml), median (range)	170 (65–800)
Prednisolone (mg/day), median (range)	4.5 (3.0–7.5)

CRP C-reactive protein, *RF* rheumatoid factor

under inverse microscopy. Flow cytometric analysis confirmed the isolated RAFLSs as a homogeneous population (>95% CD90, <2% CD14, <1% CD19, and <1% CD3 positive). Cells at passages 3–6 were used in the following experiments, and each experiment was repeated three times with different pools of RAFLSs.

Cell treatment

RAFLSs were starved with serum-free DMEM medium for 24 h. Following starving, the cells at approximately 60–80% confluence were cultured in 10% FCS–DMEM medium with or without various concentrations (10, 20, and 30 μM) of andrographolide. After incubation for 48 h, cells were collected and subjected to the following assays.

MTT assay

Cell viability was analyzed using the MTT assay. Briefly, cells were seeded in 96-well plates to a final concentration of 1×10^4 cells/well for 24 h. The cells were untreated or treated with varying concentrations of andrographolide for another 48 h as described above. Then, 20 μL of 5 mg/mL solution of MTT in PBS was added to each well. The plates were incubated for 4 h at 37°C. The precipitate was solubilized in dimethyl sulfoxide and the resulting formazan product was spectrophotometrically quantified at a wavelength of 540 nm with reference at a wavelength of 690 nm. The effect of andrographolide on cell viability was assessed as percent cell viability compared to untreated control cells, which were arbitrarily assigned 100% viability.

Cell cycle analysis

Cell cycle analysis was done by measuring DNA content using flow cytometry. Cells seeded in 6-well plates at a density of 2×10^5 cells per well were treated with or without different concentrations of andrographolide for another 48 h as described above. After the treatments, the cells were fixed, permeabilized, and stained with propidium iodide (PI; Sigma). DNA content was determined using FACSCalibur Flow Cytometer (Becton Dickinson, San Jose, CA, USA).

Apoptosis assay

Apoptosis was determined by flow cytometry with the Annexin V-FITC Apoptosis Detection Kit I (BD Biosciences) according to the manufacturer's instructions. Cells were seeded in 6-well plates (2×10^5 cells/well), and after a 24 h incubation, the cells were incubated with different concentrations of andrographolide for another 48 h as described above. After the treatments, the cells were harvested and stained with 5 μl annexin V-FITC and 10 μl PI at room temperature for 15 min in the dark. The stained cells were analyzed immediately by flow cytometry. Early apoptotic cells were defined as positive for annexin V-FITC but negative for PI staining.

Preparation of whole cell and cytosolic extracts

For preparation of whole cell extracts, cells were lysed in lysis buffer containing 1% sodium dodecyl sulfate (SDS), 0.1 mM phenylmethylsulfonyl fluoride (PMSF), and complete protease inhibitors (Roche, Mannheim, Germany). The lysates were centrifuged at 13,000×*g* for 15 min and the supernatants were frozen at −80°C until use. For preparation of cytosolic extracts, cells were suspended in five volumes of ice-cold extraction buffer containing 20 mM 4-(2-hydroxyethyl)-1-piperazineethanesulfonic acid (HEPES)/KOH (pH 7.5), 1.5 mM $MgCl_2$, 1 mM EDTA, 1 mM dithiothreitol (DTT), 0.1 mM PMSF and complete protease inhibitors. After homogenization, cell lysates were centrifuged at 1,000×*g* to discard nuclei and unbroken cells. The supernatant was centrifuged at 13,000×*g* for 15 min at 4°C to remove mitochondrial pellets. The remaining supernatant was collected as the cytosolic fraction and stored at −80°C until analysis. Protein concentrations were measured by the Bradford protein assay kit (Bio-Rad; Hercules, CA, USA) following the manufacturer's instructions.

Western blot analysis

Equal amounts (20 μg) of protein samples prepared as above were resolved by SDS–polyacrylamide gel electrophoresis and transferred onto nitrocellulose membranes. After blocking in 5% fat-free milk for 1 h at room temperature, membranes were incubated with primary antibodies followed by appropriate

secondary antibodies. Immunoreactive proteins were visualized using an enhanced chemiluminescent detection system (Amersham Biosciences; Piscataway, NJ, USA). Blots were scanned on the Fluor-S MAX MultiImager (Bio-Rad), and signal intensities were densitometrically determined using QuantityOne image software (Bio-Rad).

Caspase-3 activity assay

Intracellular caspase-3 activity was assessed by a caspase-3 colorimetric assay kit (Clonetech; Palo Alto, CA, USA) following the manufacturer's instructions. Cells seeded in 6-well plates (2×10^5 cells/well) were treated with or without andrographolide for another 48 h as described above. Cells were collected and resuspended in lysis buffer containing 50 mM HEPES, pH 7.4, 0.1% CHAPS, 1 mM DTT, 0.1 mM EDTA, and 0.1% Triton X-100. Cell lysates were centrifuged at 12,000×*g* for 10 min at 4°C. The supernatants were incubated with the reaction buffer containing 2 mM Ac-DEVD-pNA (used as the caspases 3 substrate) for 1 h at 37°C. The negative control reaction did not contain the conjugated substrate. Caspase activity was determined by measuring the absorbance at 405 nm.

Statistical analysis

Data are expressed as means±standard deviation. Statistical analysis was done using one-way analysis of variance with the Tukey's post hoc test. *P* values less than 0.05 were considered as significant.

Results

Andrographolide inhibits cell proliferation and induces cell cycle arrest in RAFLSs

To assess the effect of andrographolide on cell proliferation, RAFLSs were treated with various concentrations of andrographolide for 48 h. The MTT assay revealed that andrographolide treatment significantly decreased the proliferation of RAFLSs in a dose-dependent manner (Fig. 1a). Cell cycle analysis showed that andrographolide treatment resulted in a dose-dependent decrease in the proportion of cells in S and G2/M phases and a concomitant increase in the percentage of cells in G0/G1 phase (Fig. 1b). An approximate 30% elevation in the G0/G1 phase population and an over 50% reduction in the S- and G2/M phase fractions were seen in andrographolide (30 μM)-treated RAFLSs. These data indicates that andrographolide causes a G0/G1 cell cycle arrest in RAFLSs.

It is well-known that Cdk4 and Cdk inhibitors (p21 and p27) play crucial roles in the regulation of cell cycle progression (Harper et al. 1993; Kamura et al. 2004; Blain 2008). We next checked whether andrographolide had an influence on their expression levels. Immunoblotting analysis revealed that exposure to andrographolide caused an accumulation of p27 and p21 and a concomitant reduction of Cdk4 in comparison with untreated cells (Fig. 1c), confirming the cell cycle regulation by andrographolide.

Andrographolide induces apoptosis in RAFLSs

Next, we ascertained the effect of andrographolide on apoptosis of RAFLSs. As shown in Fig. 2, there was a concentration-dependent increase in the percentage of early apoptotic cells (defined as annexin V-positive and PI negative) in andrographolide-treated RAFLSs. Cells that were both annexin V- and PI-positive are late apoptotic cells. We found that high concentrations of andrographolide (20 and 30 μM) also caused a marked elevation in the late apoptotic population, further supporting proapoptotic activity of the compound.

Bcl-2 family proteins are important regulators of apoptosis (Adams and Cory 1998, 2001). The family comprises both antiapoptotic (e.g., Bcl-2) and proapoptotic proteins (e.g., Bax) with opposing biological functions. To explore the involvement of the Bcl-2 family members in apoptosis induced by andrographolide, the expression levels of both Bcl-2 and Bax were analyzed by Western blotting. As illustrated in Fig. 3, andrographolide treatment diminished the Bcl-2 expression and increased the Bax expression. The Bcl-2/Bax ratio was significantly decreased in andrographolide-treated RAFLSs compared to untreated cells ($P<0.01$). These results suggest that andrographolide may exert growth inhibitory effects on RAFLSs through induction of apoptosis.

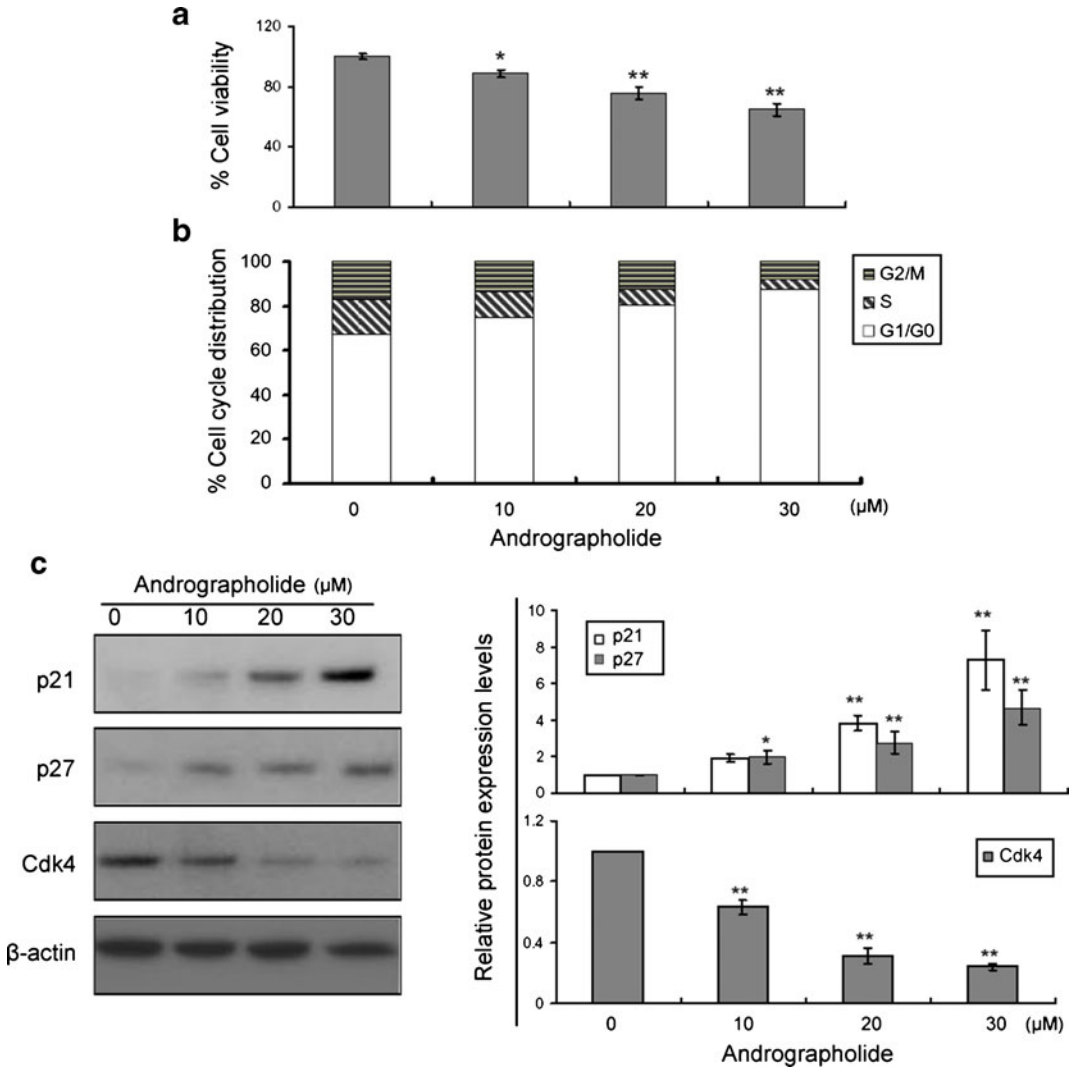

Fig. 1 Andrographolide inhibits human RAFLS proliferation through inducing G0/G1 arrest. RAFLSs were untreated or treated with different concentrations of andrographolide (10, 20, and 30 μM) for 48 h and were subjected to cell proliferation and cell cycle analysis as described in Materials and methods. **a** Andrographolide treatment interfered with the proliferation of RAFLSs in a dose-dependent manner. The results are expressed in terms of the percentage of untreated cells. Each point represents the mean±SD of three independent experiments. *$P<0.05$, **$P<0.01$ relative to untreated cells. **b** Analysis of the cell cycle distribution of andrographolide-treated RAFLSs. Results are representative of one experiment from three separate experiments with similar results. **c** Western blot analysis of p27 and Cdk4 in andrographolide-treated RAFLSs. Andrographolide treatment increased p27 expression and decreased Cdk4 expression in a dose-dependent manner. Representative blots of three independent experiments are shown in *left panels*. *Bar graphs* (*right panels*) depict densitometric analysis of the Western blots. Results are expressed relative to untreated cells set as 1. *$P<0.05$, **$P<0.01$ relative to untreated cells

Andrographolide promotes cytochrome C release and caspase-3 activation

Caspases are a family of cysteinyl aspartate-specific proteinases that play key roles in apoptosis (Nicholson and Thornberry 1997). Among them, caspase-3 is of particular interest since it is commonly activated by a number of apoptotic stimuli and has a variety of substrates (Porter and Jänicke 1999). To get more insight into the mechanism by which andrographolide induces apoptosis, we examined the expression and activity of caspases-3 in andrographolide-treated cells. Western blot analysis revealed that andrographolide treatment caused a concentration-dependent increase

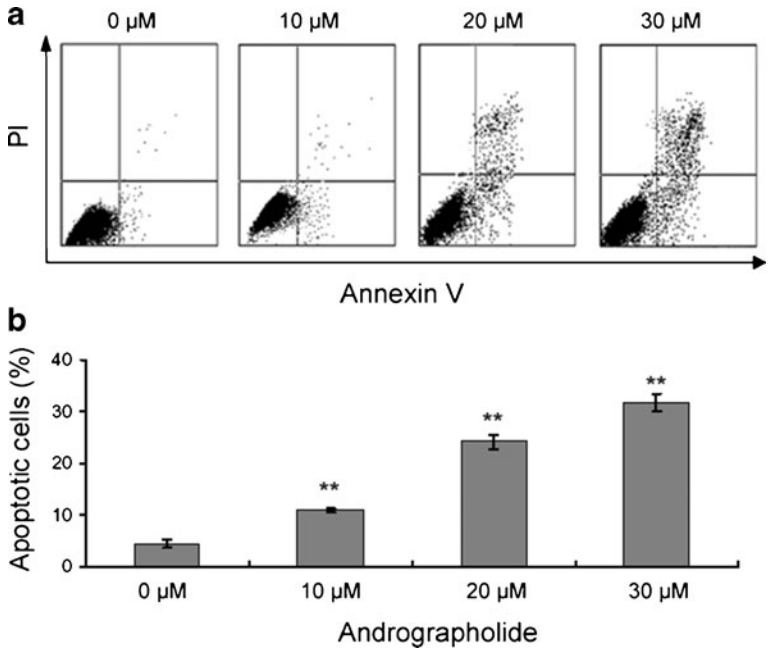

Fig. 2 Andrographolide induces apoptosis in human RAFLSs. RAFLSs were treated with different concentrations of andrographolide for 48 h and analyzed by annexin-V-FITC/PI double staining. **a** Shown are representative flow cytometry dot plots of andrographolide-treated RAFLSs. *Bar graphs* **b** represent the average percentage of apoptotic cells in each treatment group. $^{**}P<0.01$ relative to untreated cells

in the amount of cleaved caspases-3 in RAFLSs (Fig. 4a). The caspase-3 activity detected by the degradation of a fluorogenic substrate was significantly elevated in andrographolide-treated cells ($P<0.01$ relative to untreated cells; Fig. 4b).

One mechanism of caspase-3 activation involves cytochrome C, which is released from the mitochondria into the cytoplasm during apoptosis (Green and Reed 1998; Budihardjo et al. 1999). We also investigated the effect of andrographolide on cytochrome C release. Western blot analysis of the cytosolic fraction of andrographolide-treated RAFLSs revealed that andrographolide treatment resulted in a dose-dependent accumulation of cytochrome C (Fig. 4a). Taken together, these results suggest that andrographolide induces apoptotic death in RAFLSs, at least partially, through the release of cytochrome C from the mitochondria resulting in caspase-3 activation.

Discussion

Accumulating evidence indicates that FLSs are key players in the pathogenesis of RA (Müller-Ladner et

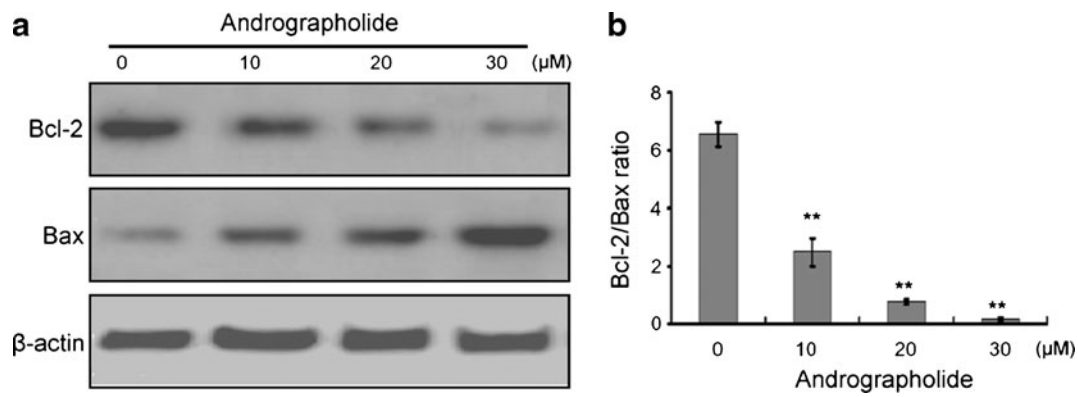

Fig. 3 Andrographolide treatment decreases the Bcl-2/Bax ratio in RAFLSs. RAFLSs treated with different concentrations of andrographolide for 48 h were assessed for Bcl-2 and Bax protein expression. **a** Shown are representative Western blots of three independent experiments. β-Actin was used as a loading control. *Bar graphs* **b** depict quantitative analysis of the Bcl-2/Bax ratio. $^{**}P<0.01$ relative to untreated cells

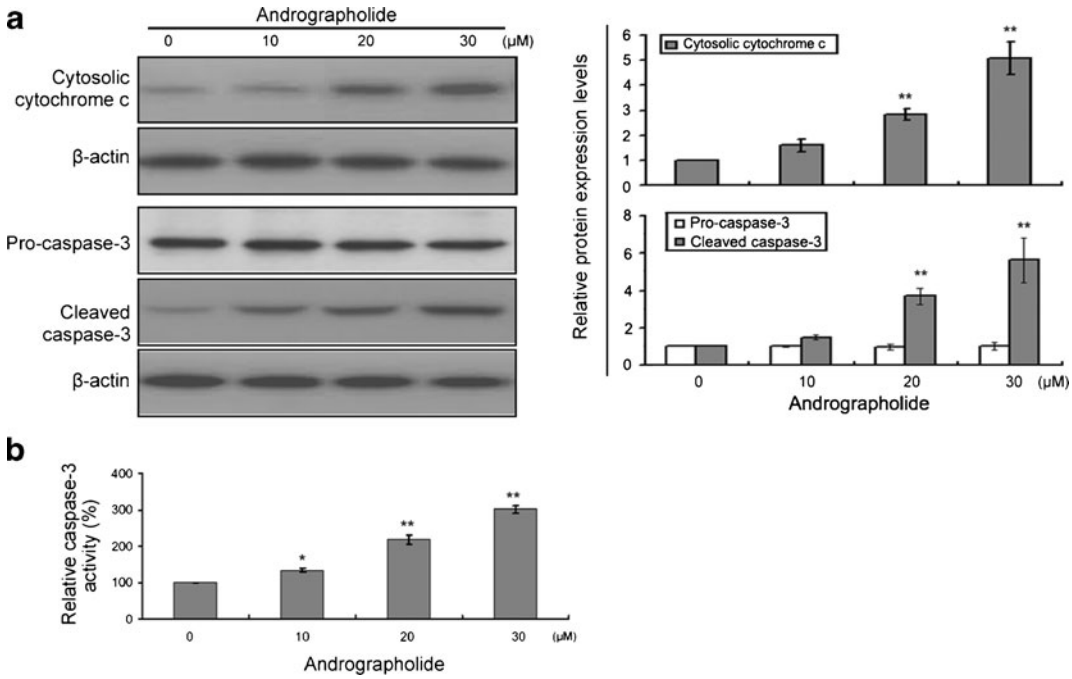

Fig. 4 Andrographolide treatment promotes cytochrome C release and caspase-3 activation in RAFLSs. RAFLSs treated with indicated concentrations of andrographolide for 48 h were subjected to Western blot analysis and caspases-3 activity assay. **a** Immunoblotting analysis of cytosolic cytochrome C and cleaved caspas-3 in andrographolide-treated RAFLSs. Detection of pro-caspase-3 was used to control for caspase-3 cleavage. β-Actin was used as loading controls. Representative blots of three independent experiments are shown in *left panels*. *Bar graphs* (*right panels*) depict densitometric analysis of the Western blots. Results are expressed relative to untreated cells set as 1. $^{**}P<0.01$ relative to untreated cells. **b** Caspases-3 activity assay. Andrographolide treatment increased caspase-3 activity in human RAFLSs in a concentration-dependent manner. Data are expressed as fold induction of caspase-3 activity relative to that in untreated cells (assigned as 100%). $^{*}P<0.05$, $^{**}P<0.01$ compared to untreated cells

al. 2007; Lefèvre et al. 2009). They actively drive inflammation and contribute to joint destruction by producing inflammatory cytokines and matrix-degrading molecules. RAFLSs have thus been proposed as therapeutic targets for this disease. In this study, we showed that andrographolide treatment inhibited the proliferation of RAFLSs in a dose-dependent manner, which is associated with induction of a G0/G1 arrest and apoptotic death. An increase of p21 and p27 expression and a concomitant decrease of Cdk4 expression were seen in andrographolide-treated cells. Exposure to andrographolide facilitated the release of cytochrome C from mitochondria and activation of caspase-3. Moreover, andrographolide-treated cells displayed a significant reduction in the Bcl-2/Bax ratio. Our data collectively suggest the therapeutic potential of andrographolide in RA.

Andrographolide is a diterpenoid lactone isolated from a traditional herbal medicine *A. paniculata*. It exhibits potent anti-inflammatory and anti-cancer activities (Bao et al. 2009; Li et al. 2009; Manikam and Stanslas 2009; Chun et al. 2010). This compound has been found to exert growth inhibitory effects on a variety of types of tumor cells (Cheung et al. 2005; Ji et al. 2007; Shi et al. 2008). Here, we extended these findings to show that andrographolide also had suppressive effects on RAFLS proliferation and induced a cell cycle arrest at the G0/G1 phase. Moreover, andrographolide-treated cells displayed the deregulation of cell cycle regulators p27, p21, and Cdk4. Upregulation of p27 is linked to induction of a G0/G1 cell cycle arrest through its interaction with cyclin–Cdk complexes (Toyoshima and Hunter 1994). Nah et al. (2009) reported that the activation of p27 and p21 contributes to the antiproliferative action of melatonin in RAFLSs. These observations provide a mechanistic explanation for the modulation of cell cycle distribution of RAFLSs by andrographolide.

Defective apoptosis of RAFLSs has been linked to the synovial hyperplasia associated with RA (Hayashi

et al. 2007; García et al. 2009, 2010). Induction of RAFLS apoptosis therefore represents a new approach for the prevention of joint destruction. It has been reported that an anti-rheumatic drug hydroxychloroquine at concentrations of 10–100 μM can facilitate the apoptosis of rheumatoid synoviocytes (Kim et al. 2006). High concentrations of simvastatin, i.e., 1.0–50 μM, were found to cause prominent apoptosis in RAFLSs in a dose-dependent manner (Yokota et al. 2008). Liagre et al. (2004) demonstrated that 40 μM diosgenin, a plant steroid, provokes marked apoptosis in human RAFLSs. Andrographolide has been documented to be an effective apoptosis inducer. It induces mitochondrial-mediated apoptosis in lymphoma cells through caspase cascades (Yang et al. 2010). Yang et al. (2009) showed that andrographolide enhances 5-fluorouracil-induced apoptosis via caspase-8-dependent mitochondrial pathway involving p53 participation in hepatocellular carcinoma cells. Notably, we found that andrographolide at concentrations of >20 μM caused apoptotic death in RAFLSs. Moreover, there was an increased release of cytochrome C from mitochondria and activation of caspase-3 in andrographolide-treated RAFLSs. Cytochrome C, a component of the mitochondrial electron transfer chain, initiates caspase activation when released from mitochondria during apoptosis. The release of cytochrome C activates the apoptotic protease activating factor, Apaf-1, which then initiates a protease cascade resulting in the activation of caspase-3 (Jiang and Wang 2004). The present findings suggest that andrographolide triggers apoptosis in RAFLSs, likely via the cytochrome C-mediated caspase activation. Nevertheless, it is still unclear to what extent the caspase-3-dependent pathway is involved in the apoptotic cell death caused by andrographolide. Further studies are needed to define the detailed apoptotic pathways involved. Lu et al. (2011) showed that andrographolide acts as a novel NF-κB inhibitor. This compound was reported to induce apoptosis in B16F-10 melanoma cells by inhibiting NF-κB-mediated Bcl-2 activation and modulating p53-induced caspase-3 gene expression (Pratheeshkumar et al. 2011). These findings raise the possibility that deregulation of the NF-κB singling cascade may be responsible for the effects of andrographolide on RAFLSs. We will address this possibility in future work. It is also of interest to determine whether andrographolide would have beneficial effects when combined with existing anti-rheumatic agents such as methotrexate (Cutolo et al. 2001) and tumor necrosis factor blockers (Saleem et al. 2010).

The release of cytochrome C and cytochrome C-mediated apoptosis are controlled by the two opposing members of the bcl-2 family, Bcl-2, and Bax. Bcl-2 interferes with the release of cytochrome C and thus caspase activation (Kluck et al. 1997), while transiently expressed Bax localizes to mitochondria and induces the release of cytochrome C, activation of caspase-3, membrane blebbing, nuclear fragmentation, and cell death (Rossé et al. 1998). Notably, we found that andrographolide treatment markedly decreased the Bcl-2 expression and increased the Bax expression in RAFLSs. The Bcl-2/Bax ratio was significantly diminished in andrographolide-treated RAFLSs in a concentration-dependent manner. These results partially explained the elevated cytochrome C production induced by andrographolide. However, the exact mechanism by which andrographolide modulates the Bcl-2/Bax ratio remains to be further elucidated. There is growing evidence that andrographolide has potent anti-inflammatory activity (Bao et al. 2009; Li et al. 2009). Since FLSs are key effector cells in RA by producing cytokines that mediate inflammation and cartilage destruction (Bartok and Firestein 2010), it is of interest to address whether andrographolide would affect the cytokine release of RAFLSs.

In summary, our data show that andrographolide treatment inhibits the proliferation of human RAFLSs through induction of a cell cycle arrest at the G0/G1 phase and enhances cytochrome C-mediated apoptosis.

References

Adams JM, Cory S. The Bcl-2 protein family: arbiters of cell survival. Science. 1998;281:1322–6.

Adams JM, Cory S. Life-or-death decisions by the Bcl-2 protein family. Trends Biochem Sci. 2001;26:61–6.

Arnett FC, Edworthy SM, Bloch DA, McShane DJ, Fries JF, Cooper NS, et al. The American Rheumatism Association 1987 revised criteria for the classification of rheumatoid arthritis. Arthritis Rheum. 1988;31:315–24.

Bao Z, Guan S, Cheng C, Wu S, Wong SH, Kemeny DM, et al. A novel antiinflammatory role for andrographolide in asthma via inhibition of the nuclear factor-kappaB pathway. Am J Respir Crit Care Med. 2009;179:657–65.

Bartok B, Firestein GS. Fibroblast-like synoviocytes: key effector cells in rheumatoid arthritis. Immunol Rev. 2010;233:233–55.

Blain SW. Switching cyclin D-Cdk4 kinase activity on and off. Cell Cycle. 2008;7:892–8.

Budihardjo I, Oliver H, Lutter M, Luo X, Wang X. Biochemical pathways of caspase activation during apoptosis. Annu Rev Cell Dev Biol. 1999;15:269–90.

Burgos RA, Hancke JL, Bertoglio JC, Aguirre V, Arriagada S, Calvo M, et al. Efficacy of an *Andrographis paniculata* composition for the relief of rheumatoid arthritis symptoms: a prospective randomized placebo-controlled trial. Clin Rheumatol. 2009;28:931–46.

Chen JX, Xue HJ, Ye WC, Fang BH, Liu YH, Yuan SH, et al. Activity of andrographolide and its derivatives against influenza virus in vivo and in vitro. Biol Pharm Bull. 2009;32:1385–91.

Cheung HY, Cheung SH, Li J, Cheung CS, Lai WP, Fong WF, et al. Andrographolide isolated from *Andrographis paniculata* induces cell cycle arrest and mitochondrial-mediated apoptosis in human leukemic HL-60 cells. Planta Med. 2005;71:1106–11.

Chun JY, Tummala R, Nadiminty N, Lou W, Liu C, Yang J, et al. Andrographolide, an herbal medicine, inhibits interleukin-6 expression and suppresses prostate cancer cell growth. Genes Cancer. 2010;1:868–76.

Cutolo M, Sulli A, Pizzorni C, Seriolo B, Straub RH. Anti-inflammatory mechanisms of methotrexate in rheumatoid arthritis. Ann Rheum Dis. 2001;60:729–35.

Firestein GS. Invasive fibroblast-like synoviocytes in rheumatoid arthritis: passive responders or transformed aggressors? Arthritis Rheum. 1996;39:1781–90.

Firestein GS. Evolving concepts of rheumatoid arthritis. Nature. 2003;423:356–61.

García S, Mera A, Gómez-Reino JJ, Conde C. Poly(ADP-ribose) polymerase suppression protects rheumatoid synovial fibroblasts from Fas-induced apoptosis. Rheumatology (Oxford). 2009;48:483–9.

García S, Liz M, Gómez-Reino JJ, Conde C. Akt activity protects rheumatoid synovial fibroblasts from Fas-induced apoptosis by inhibition of Bid cleavage. Arthritis Res Ther. 2010;12:R33.

Green DR, Reed JC. Mitochondria and apoptosis. Science. 1998;281:1309–12.

Harper JW, Adami GR, Wei N, Keyomarsi K, Elledge SJ. The p21 Cdk-interacting protein Cip1 is a potent inhibitor of G1 cyclin-dependent kinases. Cell. 1993;75:805–16.

Hayashi S, Miura Y, Nishiyama T, Mitani M, Tateishi K, Sakai Y, et al. Decoy receptor three expressed in rheumatoid synovial fibroblasts protects the cells against Fas-induced apoptosis. Arthritis Rheum. 2007;56:1067–75.

Ji L, Liu T, Liu J, Chen Y, Wang Z. Andrographolide inhibits human hepatoma-derived Hep3B cell growth through the activation of c-Jun N-terminal kinase. Planta Med. 2007;73:1397–401.

Jiang X, Wang X. Cytochrome C-mediated apoptosis. Annu Rev Biochem. 2004;73:87–106.

Kamura T, Hara T, Matsumoto M, Ishida N, Okumura F, Hatakeyama S, et al. Cytoplasmic ubiquitin ligase KPC regulates proteolysis of p27(Kip1) at G1 phase. Nat Cell Biol. 2004;6:1229–35.

Kim WU, Yoo SA, Min SY, Park SH, Koh HS, Song SW, et al. Hydroxychloroquine potentiates Fas-mediated apoptosis of rheumatoid synoviocytes. Clin Exp Immunol. 2006;144:503–11.

Kluck RM, Bossy-Wetzel E, Green DR, Newmeyer DD. The release of cytochrome C from mitochondria: a primary site for Bcl-2 regulation of apoptosis. Science. 1997;275:1132–6.

Lafyatis R, Remmers EF, Roberts AB, Yocum DE, Sporn MB, Wilder RL. Anchorage-independent growth of synoviocytes from arthritic and normal joints. Stimulation by exogenous platelet-derived growth factor and inhibition by transforming growth factor-beta and retinoids. J Clin Invest. 1989;83:1267–76.

Lefèvre S, Knedla A, Tennie C, Kampmann A, Wunrau C, Dinser R, et al. Synovial fibroblasts spread rheumatoid arthritis to unaffected joints. Nat Med. 2009;15:1414–20.

Li J, Luo L, Wang X, Liao B, Li G. Inhibition of NF-kappaB expression and allergen-induced airway inflammation in a mouse allergic asthma model by andrographolide. Cell Mol Immunol. 2009;6:381–5.

Liagre B, Vergne-Salle P, Corbiere C, Charissoux JL, Beneyt-out JL. Diosgenin, a plant steroid, induces apoptosis in human rheumatoid arthritis synoviocytes with cyclooxygenase-2 overexpression. Arthritis Res Ther. 2004;6:R373–83.

Lu WJ, Lee JJ, Chou DS, Jayakumar T, Fong TH, Hsiao G, et al. A novel role of andrographolide, an NF-kappa B inhibitor, on inhibition of platelet activation: the pivotal mechanisms of endothelial nitric oxide synthase/cyclic GMP. J Mol Med (Berl). 2011. doi:10.1007/s00109-011-0800-0.

Manikam SD, Stanslas J. Andrographolide inhibits growth of acute promyelocytic leukaemia cells by inducing retinoic acid receptor-independent cell differentiation and apoptosis. J Pharm Pharmacol. 2009;61:69–78.

Müller-Ladner U, Kriegsmann J, Franklin BN, Matsumoto S, Geiler T, Gay RE, et al. Synovial fibroblasts of patients with rheumatoid arthritis attach to and invade normal human cartilage when engrafted into SCID mice. Am J Pathol. 1996;149:1607–15.

Müller-Ladner U, Ospelt C, Gay S, Distler O, Pap T. Cells of the synovium in rheumatoid arthritis. Synovial fibroblasts. Arthritis Res Ther. 2007;9:223.

Nah SS, Won HJ, Park HJ, Ha E, Chung JH, Cho HY, et al. Melatonin inhibits human fibroblast-like synoviocyte proliferation via extracellular signal-regulated protein kinase/P21 (CIP1)/P27(KIP1) pathways. J Pineal Res. 2009;47:70–4.

Nicholson DW, Thornberry NA. Caspases: killer proteases. Trends Biochem Sci. 1997;22:299–306.

Pap T, Müller-Ladner U, Gay RE, Gay S. Fibroblast biology. Role of synovial fibroblasts in the pathogenesis of rheumatoid arthritis. Arthritis Res. 2000;2:361–7.

Pope RM. Apoptosis as a therapeutic tool in rheumatoid arthritis. Nat Rev Immunol. 2002;2:527–35.

Porter AG, Jänicke RU. Emerging roles of caspase-3 in apoptosis. Cell Death Differ. 1999;6:99–104.

Pratheeshkumar P, Sheeja K, Kuttan G. Andrographolide induces apoptosis in B16F-10 melanoma cells by inhibiting NF-κB-mediated bcl-2 activation and modulating p53-induced caspase-3 gene expression. Immunopharmacol Immunotoxicol. 2011. doi:10.3109/08923973.2011.588233.

Rossé T, Olivier R, Monney L, Rager M, Conus S, Fellay I, et al. Bcl-2 prolongs cell survival after Bax-induced release of cytochrome C. Nature. 1998;391:496–9.

Saleem B, Keen H, Goeb V, Parmar R, Nizam S, Hensor EM, et al. Patients with RA in remission on TNF blockers: when and in whom can TNF blocker therapy be stopped? Ann Rheum Dis. 2010;69:1636–42.

Shi MD, Lin HH, Lee YC, Chao JK, Lin RA, Chen JH. Inhibition of cell-cycle progression in human colorectal carcinoma Lovo cells by andrographolide. Chem Biol Interact. 2008;174:201–10.

Toyoshima H, Hunter T. p27, a novel inhibitor of G1 cyclin-Cdk protein kinase activity, is related to p21. Cell. 1994;78:67–74.

Yang L, Wu D, Luo K, Wu S, Wu P. Andrographolide enhances 5-fluorouracil-induced apoptosis via caspase-8-dependent mitochondrial pathway involving p53 participation in hepatocellular carcinoma (SMMC-7721) cells. Cancer Lett. 2009;276:180–8.

Yang S, Evens AM, Prachand S, Singh AT, Bhalla S, David K, et al. Mitochondrial-mediated apoptosis in lymphoma cells by the diterpenoid lactone andrographolide, the active component of *Andrographis paniculata*. Clin Cancer Res. 2010;16:4755–68.

Yokota K, Miyoshi F, Miyazaki T, Sato K, Yoshida Y, Asanuma Y, et al. High concentration simvastatin induces apoptosis in fibroblast-like synoviocytes from patients with rheumatoid arthritis. J Rheumatol. 2008;35:193–200.